Appl. Magn. Reson. 10, 71–86 (1996)

Applied Magnetic Resonance

A Systematic Approach for Studying Cu Imidazole Interactions Using Multi-Frequency ESEEM: Application to Cu(II)-Bleomycin and Model Systems

P. J. van Dam[1], E. J. Reijerse[1], M. J. van der Meer[1], R. Guajardo[2], P. K. Mascharak[2], and E. de Boer[1]

[1] Department of Molecular Spectroscopy, University of Nijmegen, Nijmegen, The Netherlands
[2] Department of Chemistry and Biochemistry, University of California at Santa Cruz, USA

Received June 19, 1995

Abstract. Many copper containing proteins exhibit well defined ESEEM signals detected at X-band and C-band. In these systems the Cu(II) ion is coordinated to one or several histidine residues. The main sharp features measured in the ESEEM spectra originate from the interaction of the unpaired electron with the remote nitrogen nucleus of the histidine ring. The relative intensities of these features contain information about the orientation of the NQI-tensor in the molecular axis frame as defined by the principal axes of the *g*-matrix. This information can be related to the orientation of the imidazole ring in the complex. We present a systematic approach to determine the constraints of the Euler angles α, β, γ of the NQI-tensor in the *g*-matrix principal axis system. The first step is to analyze the intensity ratios of the quadrupole peaks and the line shape of the double quantum feature measured on the canonical positions in the EPR spectrum. This will lead to a constraint in the angles (α, β) as well as the effective hyperfine interaction. This information is further refined using spectra on other orientation selective positions. We have applied this method to Cu(II)-Bleomycin and two model compounds: Cu(II)-Pypep and Cu(II)-PMA of which we have determined the principal quadrupole values and the orientation of the quadrupole tensor with respect to the *g*-matrix axis system.

1. Introduction

Bleomycin (BLM) belongs to a group of metallo-glycopeptide antibiotics used in the treatment of certain tumours. It is isolated from cultures of *Streptomyces verticillus* as a copper(II)-complex. The action mechanism involves the formation of an activated Fe(II)Bleomycin complex with oxygen that is capable of binding to and cleaving intracellular DNA [1]. Since it was discovered in 1966 by Umezawa [2] a great deal of research has been done on the action mechanism of bleomycin, but a structure in solution has not yet been established. The most common BLM, Bleomycin-A_2, has a bithiazole-γ-aminopropyl dimethyl sulfonium tail that can bind to the minor groove of the DNA. The other part,

containing the metal complex, consists of a sugar chain, a pyrimidyl-propionamide, a β-aminoalanine, and a β-hydroxyhistidine group (see Fig. 1). Iitaka *et al.* [3] was able to derive the X-ray structure of Cu(II)-P-3A, a biosynthetic precursor of BLM that lacks the sugar and bithiazole side chains. 2D-NMR measurements by Akkermans *et al.* [4–6] suggested, however, that the sugar chain is involved in the metal binding.

Burger *et al.* [7] applied the ESEEM technique to several BLM complexes in order to obtain information about the nitrogens involved in the metal coordination. For the copper complex a characteristic pattern was obtained indicating histidine coordination. In this case only the remote (non-coordinating) ^{14}N-nucleus contributes to the ESEEM signal. For the Fe(III)-complex the situation was much more complicated. All directly coordinating imino and amino nitrogens are likely to contribute to the ESEEM signal, including the aminogroup of the sugar chain, thus leading to a rich but uninterpretable ESEEM spectrum. In order to simplify the situation, we decided to study a series of model complexes (Fig. 2) containing a varying number of coordinating nitrogens. At the same time, these complexes mimic the metal binding part of BLM quite accurately [8, 9].

The first step in the characterization of these complexes is to establish the orientation of the imidazole ring using the ESEEM signal of the remote nitrogen in the copper complexes and to relate this information to the available X-ray structures.

Several groups [10–12] have demonstrated the power of ESEEM in characterizing the Cu(II)-imidazole interaction in terms of the nuclear quadrupole interac-

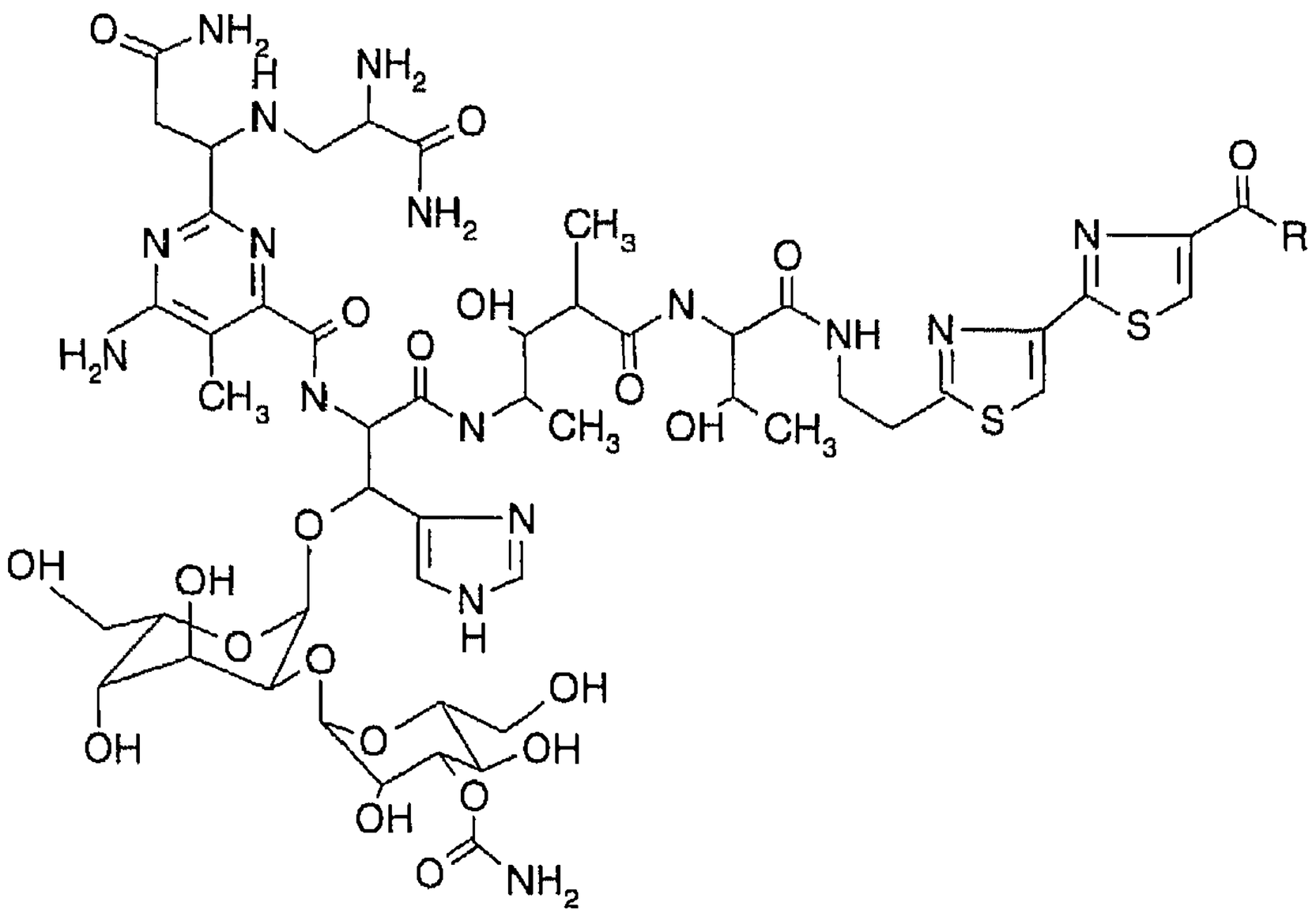

Fig. 1. The structure of Bleomycin. The terminal amine R is CH_2-$C(NH_2)H$-CO-NH_2. Nitrogens from the pyrimidine and the imidazole ring are involved in the metal coordination.

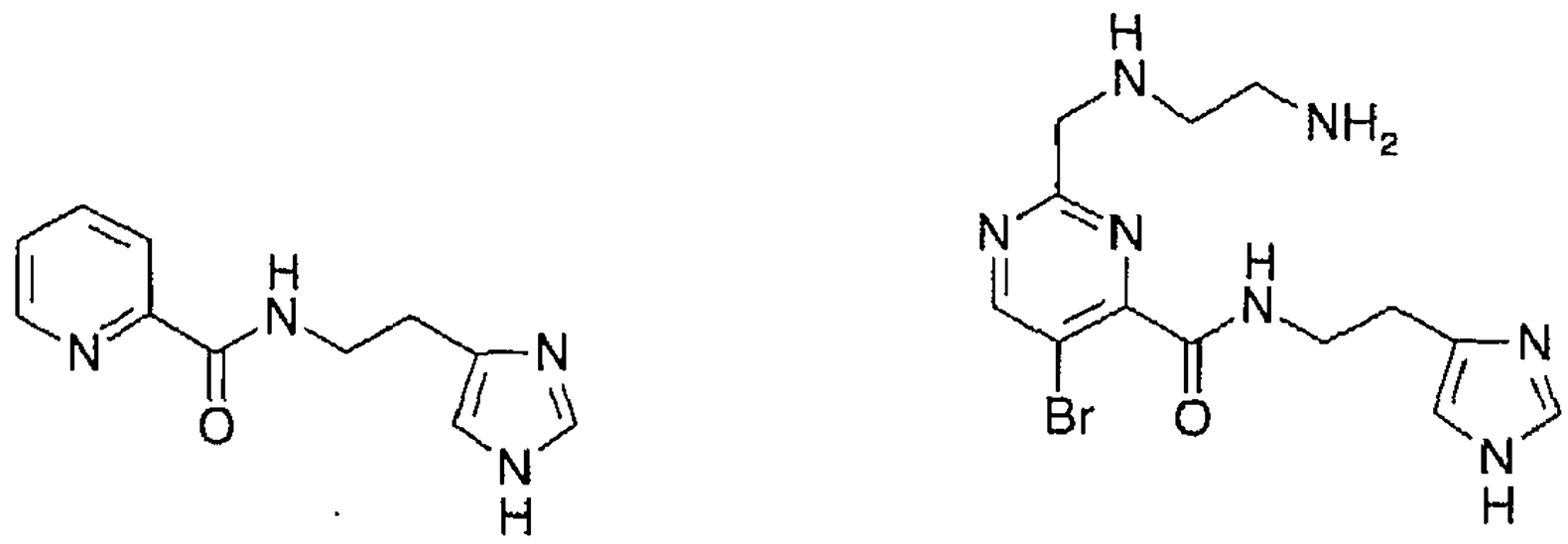

Fig. 2. The structure of the synthetic ligands PypepH (left) and PMAH (right).

tion (NQI) parameters and the (isotropic) hyperfine interaction. The extraction of the additional anisotropic parameters (Euler angles, *A*-tensor components), however, proves to be non-trivial. In this communication we present a systematic approach for the determination of the orientation of the NQI-tensor in the *g*-matrix axis frame. The strategy is applied in the analysis of the ESEEM of BLM and its various copper model complexes.

2. Experimental

Cu(II)-Bleomycin was prepared by mixing a 40 mM copper(II)acetate (Baker Reagents) solution in water with a 60 mM Bleomycin-A_2 sulphate (Nippon Kayaku co. ltd.) solution in water. After complexation an equal volume of glycerol was added to form a glass upon freezing. Samples of the model compounds Cu(II)-Pypep and Cu(II)-PMA [8, 9] (see Fig. 2) were prepared by dissolving the crystals into a water/glycerol (1 : 1) solvent. The final concentration was 10 mM. Samples were stored and measured in sealed quartz tubes.

C-band pulse experiments were performed on our home build spectrometer described elsewhere [13]. Between 7 and 9 GHz microwave pulses were amplified with a high power Litton 624 TWT amplifier. For low frequency pulses an Applied Systems Engineering broadband (2–8 GHz) TWT was used. For the X-band measurements a Bruker ESP380 spectrometer was used equipped with the variable *Q* dielectric resonator. This resonator was also used in the critically coupled mode for the CW measurements.

The three pulse ESEEM sequence ($\pi/2$–τ–$\pi/2$–T–$\pi/2$–τ–echo) was used in all experiments with phasecycling [14] to remove unwanted echoes. Echo envelope modulation decays were treated with a third order baseline correction and a hamming window apodization followed by zero filling prior to fast Fourier transformation. All data are presented as magnitude spectra.

A temperature of 10 K was obtained and controlled using an Oxford CF200 flow cryostat for the C-band setup and for the X-band measurements the Oxford CF935 flow cryostat.

3. Theory

It has been well established that the position the sharp nitrogen ESEEM features of Cu-imidazole complexes can be described using very simple analytical expressions derived for the case of "exact cancellation" [15, 16]. This regime holds when the mainly isotropic hyperfine interaction of the remote nitrogen cancels the Zeeman interaction in one of the M_S manifolds leaving only the nuclear quadrupole interaction to split the nuclear spin levels. In the "uncancelled" M_S manifold, the nuclear Zeeman interaction is reinforced by the hyperfine coupling leading to a nuclear spin sub-Hamiltonian dominated by Zeeman terms and the NQI behaving as a perturbation. The spin Hamiltonian in the strong field approximation can be expressed in terms of an electron spin contribution $\mathscr{H}_e$ and a nuclear spin contribution $\mathscr{H}_n(\pm)$:

$$\mathscr{H} = \mathscr{H}_e + \mathscr{H}_n(\pm) \tag{1}$$

with

$$\mathscr{H}_e = g\beta\, \mathbf{B}_0 \cdot \mathbf{S} \tag{2}$$

and

$$\mathscr{H}_n(\pm) = -\gamma\hbar\, \mathbf{B}_0 \cdot \mathbf{I} + A\langle \mathbf{S} \rangle_{\pm} \cdot \mathbf{I} + \mathbf{I} \cdot \mathbf{Q} \cdot \mathbf{I} \ . \tag{3}$$

In this preliminary analysis, the hyperfine interaction A is assumed to be isotropic. The first two terms of $\mathscr{H}_n$ can be combined into a Zeeman Hamiltonian:

$$\mathscr{H}_{ne}(\pm) = -\gamma\hbar \left(\mathbf{B}_0 \mp \frac{A}{2}\left(\frac{1}{\gamma h}\right)\right) \mathbf{k} \cdot \mathbf{I} \ , \tag{4}$$

where $\mathbf{k}$ represents the direction of the external magnetic field. The last term in Eq. (3) represents the NQI Hamiltonian $\mathscr{H}_{nq}$:

$$\mathscr{H}_{nq} = K(1-\eta) I_x^2 + K(1+\eta) I_y^2 - 2K I_z^2 \ . \tag{5}$$

The nuclear spin levels of the cancelled manifold are thus only determined by $\mathscr{H}_{nq}$ leading to the nuclear spin transition frequencies: $2K\eta$, $K(3+\eta)$, and $K(3-\eta)$ which emerge as sharp features in the ESEEM spectra. From the uncancelled manifold only the "double quantum" transition is usually observable:

$$\nu_{dq} = 2\left[\left(\nu_I \pm \frac{A_{iso}}{2}\right)^2 + K^2(3+\eta^2)\right]^{1/2} \ . \tag{6}$$

It has been demonstrated by Singel *et al.* [10, 15] that the intensities of the NQI signals from the cancelled M_S manifold are "polarized" with respect to the

orientation of the magnetic field. When the magnetic field is oriented along one of the principal quadrupole axes, only one of the NQI frequencies has a non-zero modulation intensity:

$$\nu_{qz} = 2K\eta \ , \qquad \nu_{qx} = K(3+\eta) \ , \qquad \nu_{qy} = K(3-\eta) \ . \tag{7}$$

In other words: peaks at x, y and z are only visible when the magnetic field is oriented along the x-, y- and z-axis, respectively. An interesting application of this behaviour would be to analyze the ESEEM spectra at a canonical position in the EPR spectrum, thus yielding information about the polar angles of the selected orientation within the NQI axis system. It would be an ideal situation if the relative intensities of the NQI signals would reflect the direction cosines of the selected orientation. The modulation intensity of the NQI lines can be conveniently calculated if we assume that the spin eigenfunctions in the uncancelled manifold are completely described by $\mathscr{H}_{ne}(-)$ treating the NQI as a first order perturbation. The spin eigenfunctions in both manifolds are then available in analytical form. Applying the expressions of Mims [17, 18], we arrive at the following results for the case where the magnetic field is oriented in the XZ-plane of the NQI axis frame, making an angle β with the z-axis:

$$\nu_{qz} = 2K\eta \ , \qquad \chi_z = \frac{1}{3}\cos^2\beta \ , \tag{8}$$

$$\nu_{qx} = K(3+\eta) \ , \qquad \chi_x = \frac{1}{3}\sin^2\beta \ , \tag{9}$$

$$\nu_{qy} = K(3-\eta) \ , \qquad \chi_y = \sin^2\beta\cos^2\beta \ , \tag{10}$$

in which χ_x, χ_y and χ_z are the modulation intensities of ν_x, ν_y and ν_z, respectively. With the magnetic field in the plane bisecting the XY-plane, the intensity of the z-polarized signal is, e.g., described as:

$$\chi_z = \frac{1}{6}\left(1+\cos^4\beta+\frac{1}{2}\sin^4\beta\right) \ . \tag{11}$$

It is clear that for arbitrary orientations the NQI intensities do not reflect the values of the direction cosines of the field vector. A unique determination of the field vector from the NQI intensities, e.g., at the $\|$-position of the Cu-imidazole spectrum is, therefore, not feasible. Only constraints for the NQI-tensor Euler angles α and β, assuming an axial g-matrix, can be estimated. In order to test this idea, we performed some model calculations. A compact representation of the correspondence between the spectra simulated for different values of α, β is obtained by treating every spectrum $\mathbf{S}(\alpha, \beta)$ as a vector. The correspondence between two spectra $\mathbf{S}(\alpha, \beta)_i$ and $\mathbf{S}(\alpha, \beta)_j$ is simply the inproduct $\mathbf{S}_i \cdot \mathbf{S}_j$ of the normalized spectrum vectors.

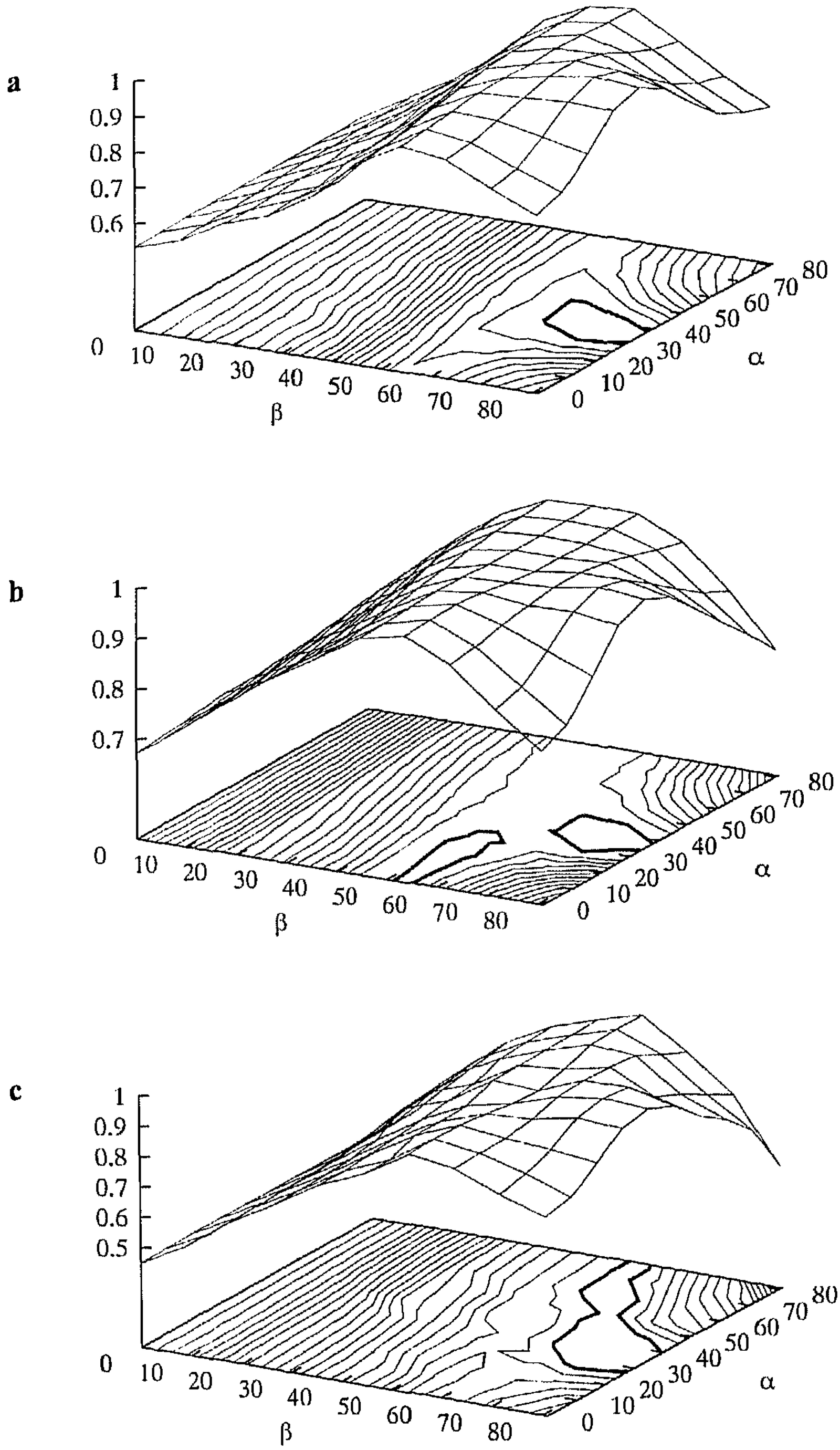

Fig. 3. Error profiles obtained by taking the inproducts of a model ESEEM spectrum with a series of simulated spectra, varying the Euler angles α and β of the NQI tensor. Parameters of the model spectrum: g-values: $g_x = 1.98$, $g_y = 1.98$ and $g_z = 2.407$, field: 230 mT ($\parallel$-position), microwave frequency: $\nu = 7.750$ GHz, pulse excitation width (Gaussian): $\Delta\nu = 100$ MHz, nitrogen quadrupole interaction: $K = 0.48 \cdot 10^{-4}$ cm^{-1}, $\eta = 0.83$, Euler angles: $\alpha = 36°$, $\beta = 72°$. The simulated spectra had identical parameters except that the Euler angles α and β were varied from 0° to 90°. Three values for A_{iso} were used: **a** $A_{iso} = 0.57 \cdot 10^{-4}$ cm^{-1}, **b** $A_{iso} = 0.47 \cdot 10^{-4}$ cm^{-1} (exact cancellation) and **c** $A_{iso} = 0.37 \cdot 10^{-4}$ cm^{-1}. The area within the bold lines indicates where the error $\varepsilon_{\alpha\beta}$ is about unity.

A model spectrum $\mathbf{S}_m$ was generated using typical parameters for copper imidazole complexes ($K = 0.12 \cdot 10^{-4}$ cm^{-1}, $\eta = 0.9$) and arbitrary values for the Euler angles ($\alpha = 72°$ and $\beta = 36°$). In Figs. 3a–3c the "error profile" ($\varepsilon_{\alpha\beta} = \mathbf{S}_m \cdot \mathbf{S}_{\alpha\beta}$) is displayed. It turns out that for the case of exact cancellation (Fig. 3b), an extended $\alpha\beta$ region gives a favourable error response (see the area within the solid contour lines where $\varepsilon_{\alpha\beta} \approx 1$). The region can be narrowed down substantially by leaving the exact cancellation condition (see Figs. 3a and 3c)! Intensity analysis using error-profiles like in Fig. 3, seems very useful for Cu-imidazole type complexes not necessarily at exact cancellation. The following strategy can be proposed:

1. Determination of K, η, A_{xx}, A_{yy}, and A_{zz} using the sharp features in the orientation selective ESEEM spectra.
2. Calculation of the α, β error profile on the $\parallel$-position (see, e.g., Fig. 3).
3. For several α, β combinations one can try to optimize the γ angle.
4. Refinement of K, η, A_x, A_y, A_z.

The proposed strategy has been applied to the orientation selective series of ESEEM spectra measured from Cu-Bleomycin and two of its model compounds (Figs. 1 and 2).

4. Results

All three compounds have a typical axial copper CW EPR spectrum with only a minor rhombic distortion. The parameters of the g-matrix and hyperfine interaction derived directly from the spectra of the compounds studied are summarized in Table 1. Simulations of the CW spectra of Cu(II)BLM and model compounds reveals a small g-anisotropy at the $g_\perp$-position. The deviation between g_x and g_y was less than 0.03. Because of the substantial excitation linewidth of the microwave pulses this deviation is too small to have any influence on the orientation selective ESEEM spectra. Fig. 4 shows a typical CW-EPR spectrum of Cu(II)-Pypep in combination with a simulation.

When the ESEEM spectra are taken at different microwave frequencies the "exact cancellation" condition is manifested by several different features. Away from exact cancellation there will be line broadening of the peaks of the cancelled manifold due to the contribution of the effective Zeeman interaction in

Table 1. The CW EPR parameters of the copper compounds.

	$g_\perp$	$g_\parallel$	$A_\perp$ (MHz)	$A_\parallel$ (MHz)
Cu(II)-Bleomycin	2.036	2.205	—	555
Cu(II)-Pypep	2.05	2.24	—	567
Cu(II)-PMA	2.05	2.22	—	531

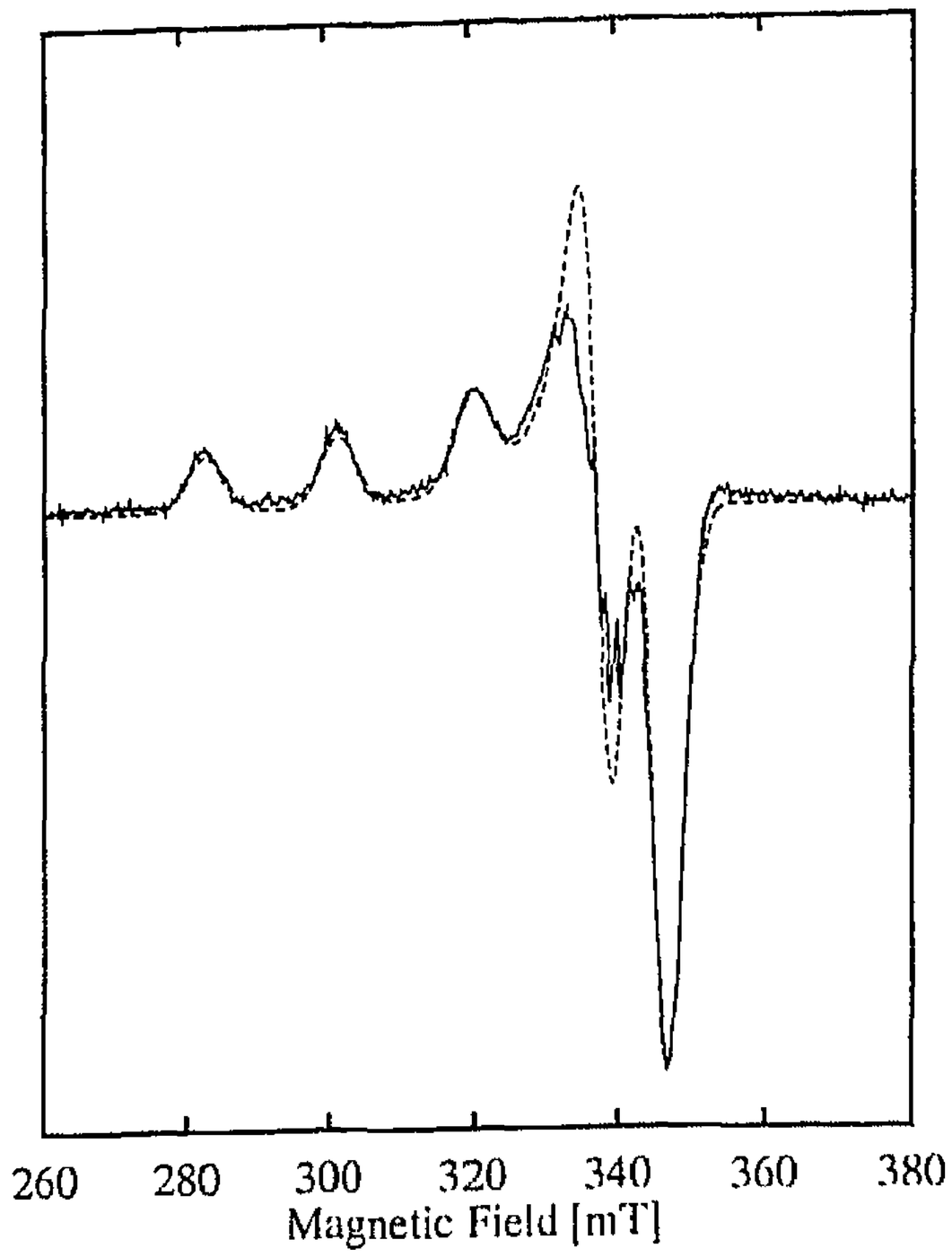

Fig. 4. A typical CW-EPR spectrum of Cu(II)-Pypep (continuous line) and the simulation (dashed line). The spectrum was simulated with g-matrix values: $g_x = 2.040$, $g_y = 2.070$ and $g_z = 2.240$. Other experimental parameters: temperature 10 K, frequency 9.727 GHz.

combination with the NQI. The effective Zeeman interaction will also lead to a shift of the ν_+ to higher frequency.

Figure 5 shows a series of three pulse ESEEM spectra of Cu(II)-BLM taken at the $\perp$-position of the EPR spectrum, for four different microwave frequencies. The above described behaviour is nicely represented in these spectra. Clearly, between 6.9 and 7.7 GHz, the resolution of the NQI peaks is optimal and the ν_+ peak has its lowest position.

Due to the anisotropy of the HFI (apparent from the doublet structure of the ν_{dq} feature) there is, of course, not a single microwave frequency for which exact cancellation is attained. It has been demonstrated, however, that the position of the NQI peaks is relatively insensitive to slight deviations from exact cancellation and the anisotropy of the HFI [16]. The K and η parameters can therefore be conveniently extracted from the spectra. Using Eq. (6), one can interpret the doublet positions of ν_{dq} in terms of the effective hyperfine components A_{xx} and A_{yy}. Spectra taken at the $\parallel$-position (not shown) show a single lineshape for the ν_{dq} peak. Again Eq. (6) was used to estimate the A_{zz} component. The resulting parameters are presented in Table 2. Due to the strongly overlapping EPR hyperfine features one cannot exclude the possibility that the second ^{14}N hyperfine component measured at the perpendicular position arises from residual orientation selection of the parallel component. In the refinement of the hyperfine parameters all components were, therefore, varied.

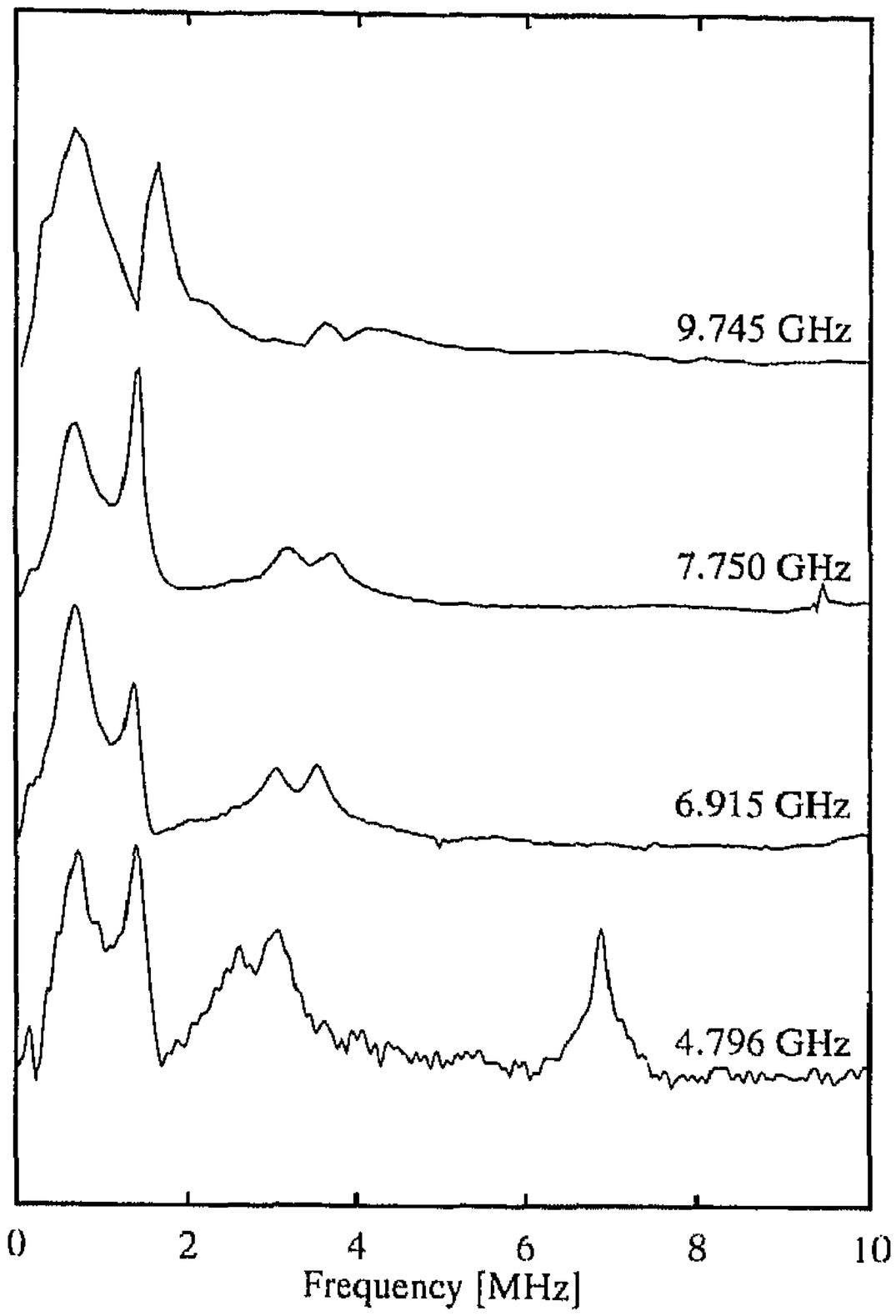

Fig. 5. Three pulse ESEEM spectra of Cu(II)-Bleomycin at different frequencies. All spectra were taken at the $g_\perp$ position at a temperature of 10 K. Experimental settings: 4.796 GHz: $B = 182$ mT, $\tau = 300$ ns; 6.915 GHz: $B = 233$ mT, $\tau = 300$ ns; 7.75 GHz: $B = 266$ mT, $\tau = 347$ ns; 9.745 GHz: $B = 315$ mT, $\tau = 240$ ns.

The anisotropy of the HFI has, however, a positive contribution in our case. At the $\perp$-position the estimated magnetic field for which the HFI is cancelled is about 280 mT for Cu(II)-PMA and Cu(II)-BLM and 330 mT for Cu(II)-Pypep. The lower A_{zz} value will lead to a lower field for "exact cancellation". (About 230 mT for Cu(II)-PMA and Cu(II)-BLM and 290 mT for Cu(II)-Pypep.) Thus, if we choose the right microwave frequency for cancellation at the $\perp$-position there will be in the same spectrum also cancellation at the $\parallel$-position!

Table 2. Hyperfine and quadrupole parameters of the remote nitrogen estimated from the ESEEM spectra.

	$K = e^2qQ/4h$ (MHz)	η	A_{xx} (MHz)	A_{yy} (MHz)	A_{zz} (MHz)
Cu(II)-Bleomycin	0.35	0.9	1.75	1.22	1.22
Cu(II)-Pypep	0.36	0.89	2.04	1.55	1.55
Cu(II)-PMA	0.39	0.74	1.76	1.20	1.20

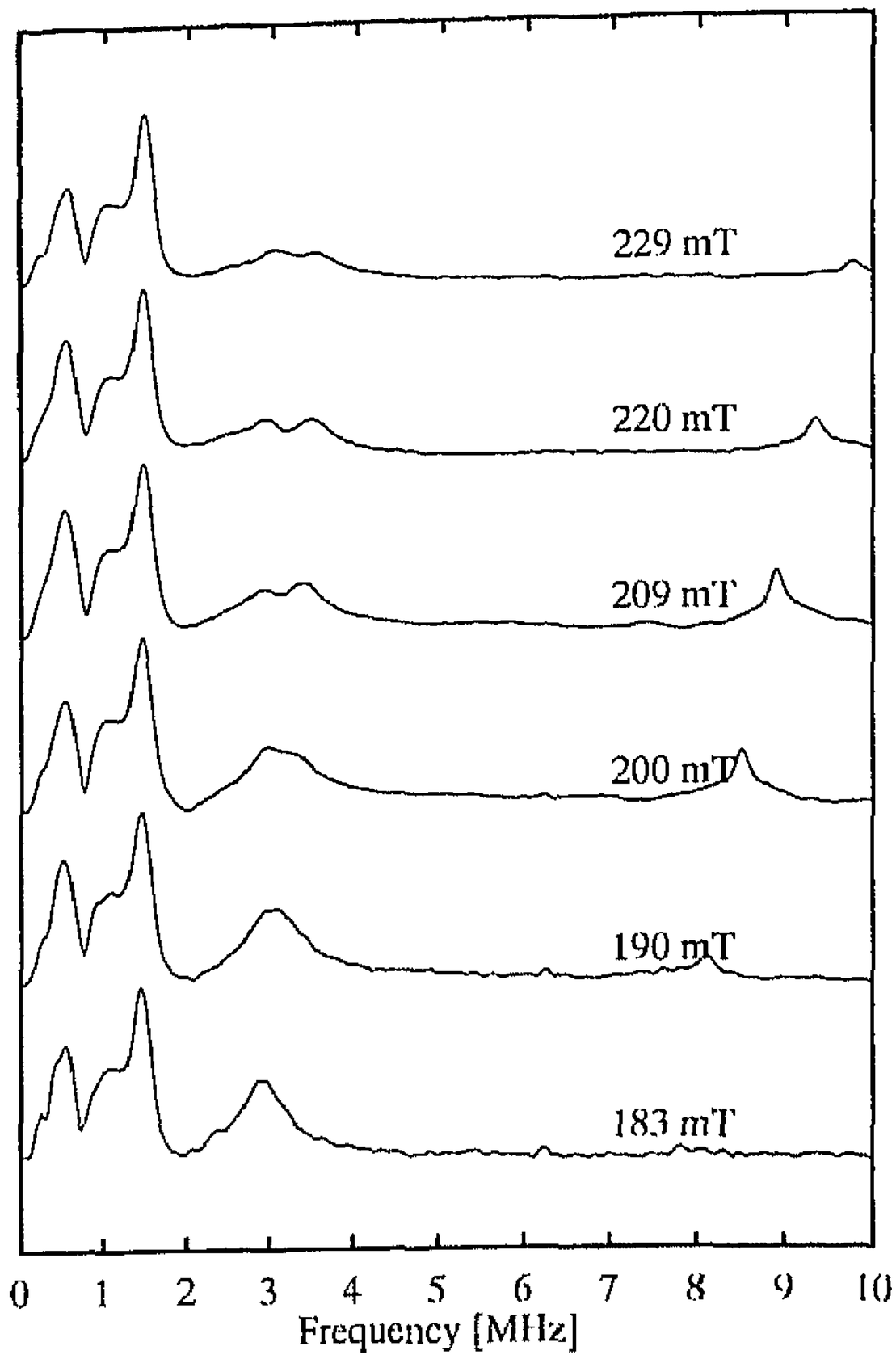

Fig. 6. C-band ESEEM (three pulse) spectra of Cu(II)-PMA recorded at different field positions. Temperature 10 K, frequency 6.487 GHz, $\tau = 350$ ns, repetition time 2 ms.

Orientation selective ESEEM series of Cu(II)-PMA, Cu(II)-Pypep and Cu(II)-BLM are presented in Figs. 6, 8 and 9. All spectra have virtually identical features indicating the close similarity of the complexes. The estimated spectral parameters (K, η, A_{xx}, A_{yy} and A_{zz}) collected in Table 2 are typical for a distant protonated imidazole nitrogen near exact cancellation.

4.1. Simulations

The ESEEM spectra of all compounds were analyzed following the strategy outlined above. The modulation expressions of Mims [17, 18] were used as implemented in MAGRES [19]. Due to the high asymmetry parameter η, the ν_0 and the ν_- peak overlap, making it difficult to obtain correct peak heights or to separate all three ESEEM lines of the cancelled manifold. Therefore we have chosen not to use the ratio of peak heights as has been done before [10] but to compare the spectra directly. For that purpose we have treated the measured spectrum and the simulation as a vector and took the inproduct between those vectors. Since our computer program is searching for the minima not $\varepsilon_{\alpha\beta}$ is

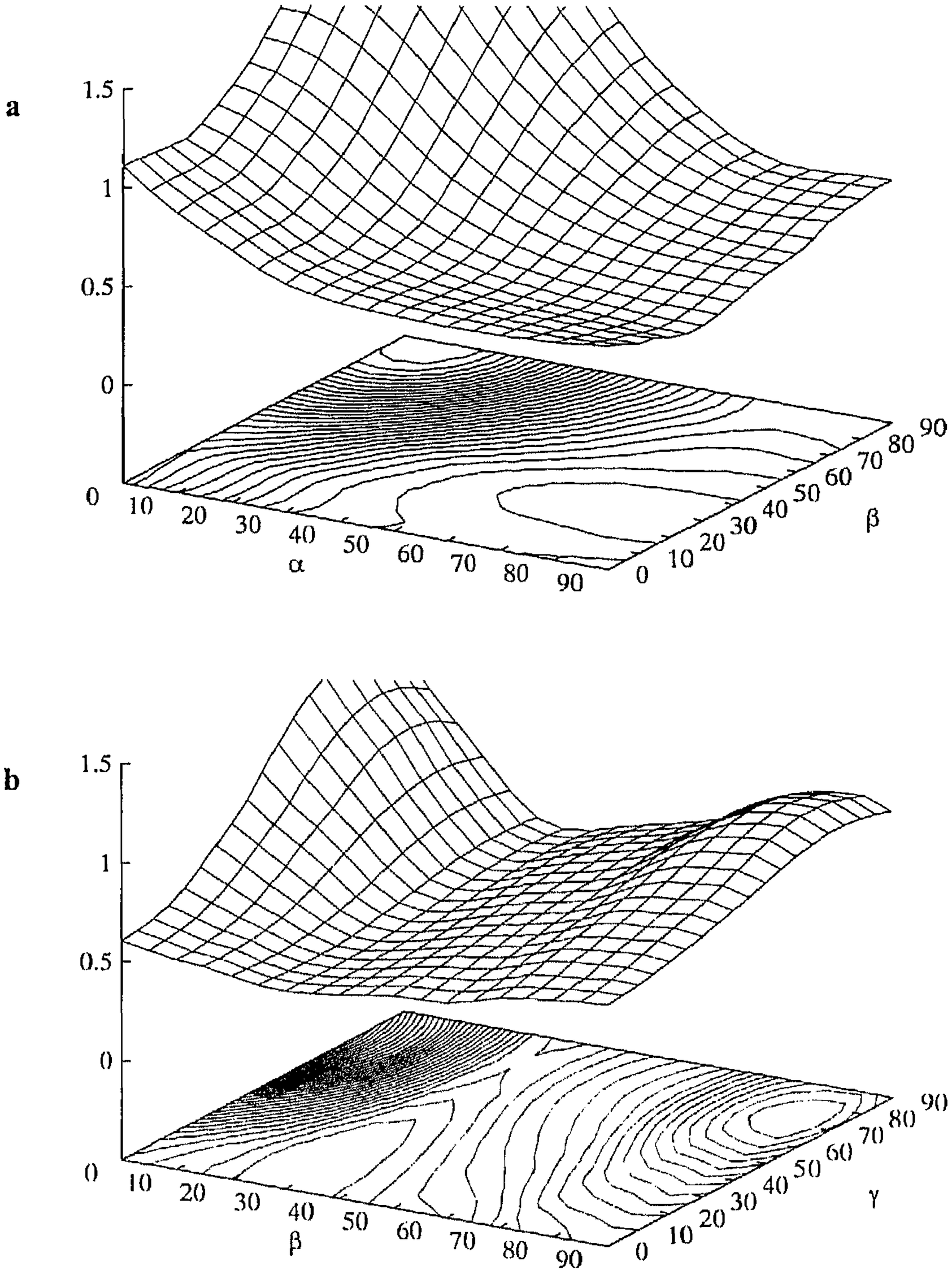

Fig. 7. Inverse inproduct profiles of simulations and measurements of Cu(II)-PMA as a function of the Euler angles between the *g*-matrix and the NQI tensor. For the spectral inproducts only the lines of the cancelled manifold are taken into account (see text).

calculated but the inverse of it. Thus a perfect fit will lead to a value of unity and deviations between simulation and measurement will result into a proportional smaller value.

The inverse inproduct, summed over all ESEEM spectra in the orientation selective series of Cu(II)-PMA (Fig. 6), were taken with the corresponding simulated spectra as a function of Euler angles α, β, and γ. The fixed simulation parame-

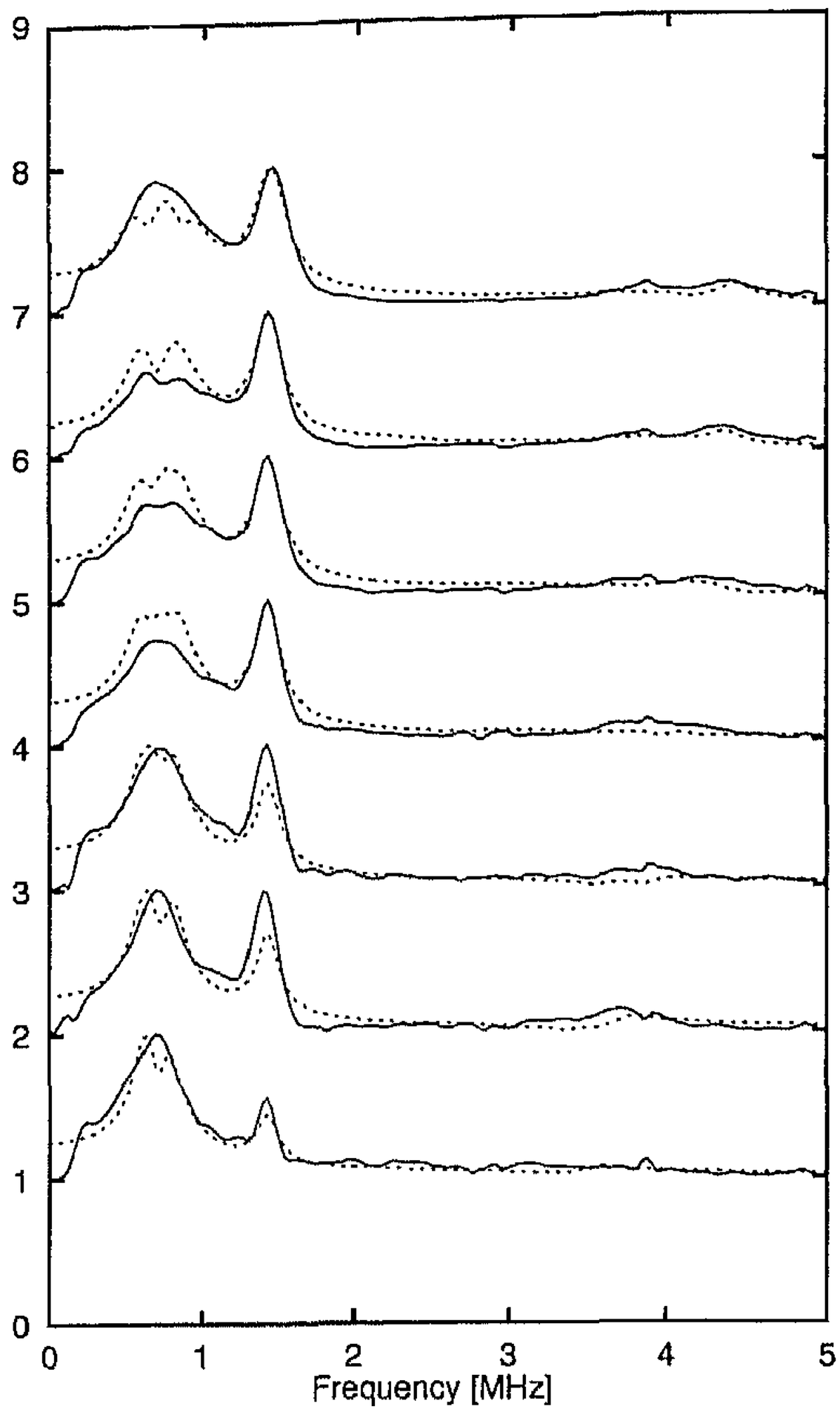

Fig. 8. Complete simulation (dashed lines) of the Cu(II)-Pypep ESEEM spectra (solid lines) with $\tau = 160$ ns at 9.747 GHz. Now the hyperfine interaction has been adjusted to rhombic values: $A_x = 2.1$ MHz, $A_y = 1.65$ MHz and $A_z = 1.5$ MHz; $P_x = 0.04$ MHz, $P_y = 0.66$ MHz and $P_z = -0.70$ MHz. The Euler angles are $\alpha = 115°$, $\beta = 26°$ and $\gamma = 70°$.

ters were taken from Tables 1 and 2. Fig. 7a shows the profile as a function of α, β ($\gamma = 0$). The best α value was selected and a second profile was calculated as a function of β, γ (Fig. 7b). Several profiles were calculated fixing α, β and γ at certain values. As can be observed in Fig. 7, the value of γ cannot be determined very accurately. This is to be expected since the anisotropy in the *xy*-plane of the metal complex is only determined by the ^{14}N-HFI components (Table 2) which have only minor influence on the intensity and shape of the NQI features. The parameters were further refined by concentrating on the lineshape of the ν_{dq} feature. To match its intensity and shape, it proved necessary to introduce a rhombic component in the ^{14}N-HFI. Fig. 8 shows the "best-fit" results for Cu(II)-Pypep, while in Fig. 9 the fit patterns for Cu(II)-BLM are presented. Clearly, the Cu(II)-BLM results are quite convincing. The fit for Cu(II)-Pypep is somewhat less accurate, although the general pattern of intensity variations over the orientation selective series is nicely reflected in the simulations.

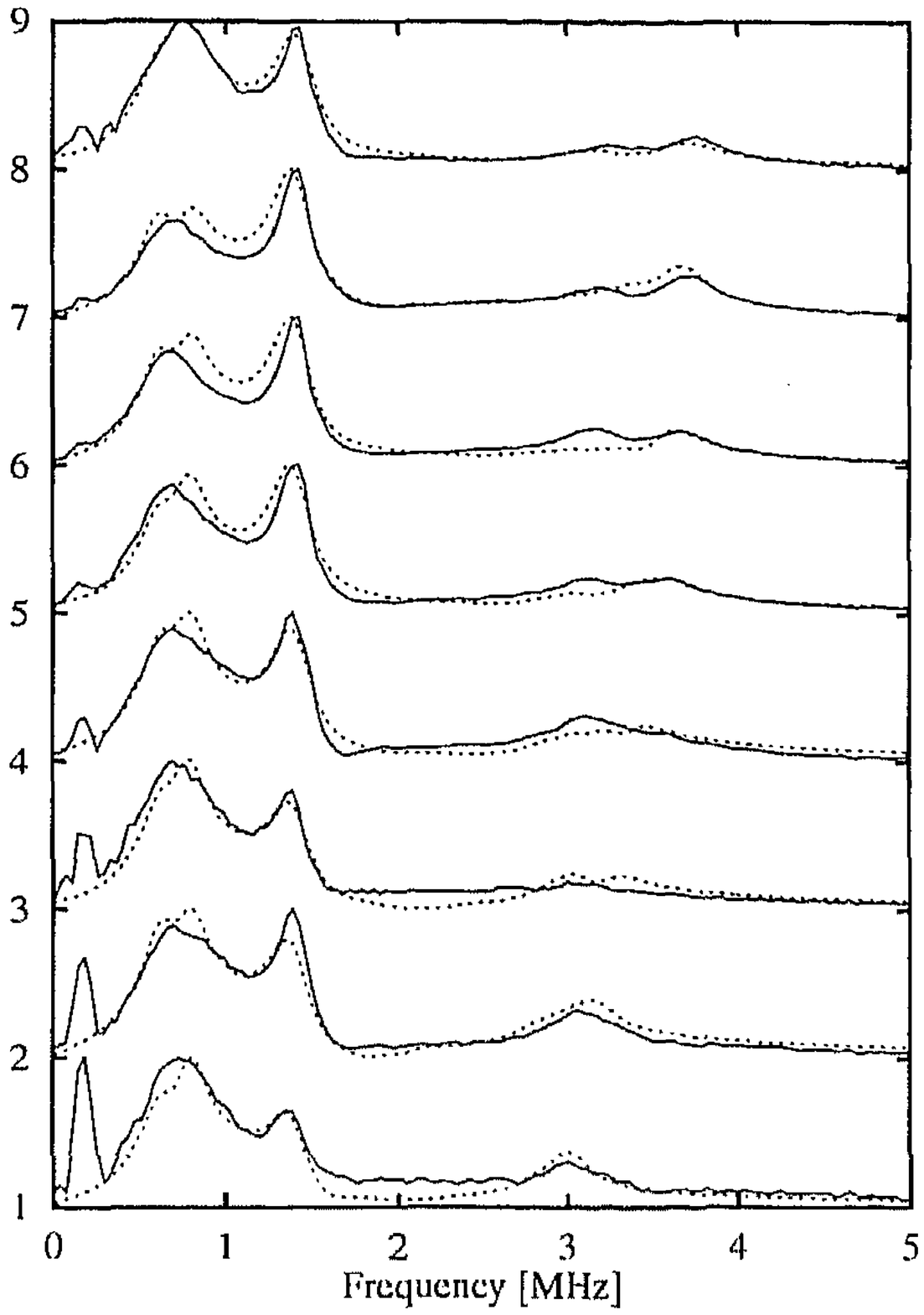

Fig. 9. Complete simulation (dashed lines) of the Cu(II)-Bleomycin ESEEM spectra (solid lines) with $\tau = 347$ ns at 7.750 GHz. Also with a rhombic A-tensor: $A_x = 1.74$ MHz, $A_y = 1.44$ MHz and $A_z = 1.23$ MHz; $P_x = 0.04$ MHz, $P_y = 0.67$ MHz and $P_z = -0.71$ MHz. The Euler angles are $\alpha = 120°$, $\beta = 36°$ and $\gamma = 78°$.

One should realize that many parameters which are difficult to access, still influence the spectra. The effect of the finite pulse-length leads to inaccuracy of the simulation parameters for the dead-time and the τ-values. These variations

Table 3. The Euler angles defining the orientation of the NQI tensor in the molecular frame are compared with the equivalent angles derived from the crystallographic data [9, 22].

	From simulations		Crystallographic data	
	α	β	α	β
Cu(II)-Bleomycin	120	36		
Cu(II)-Pypep	115	26	44	22
Cu(II)-PMA[1]	90	35	3	22
Cu(II)-PMA[2]	90	35	20	29

[1] $g_{\|}$ in the direction of the axial nitrogen.
[2] $g_{\|}$ perpendicular to the coordinating plane.

can have a substantial effect on the ESEEM lineshapes. In addition, the effect of the HFI-tensor orientation is equally difficult to access. Extensive "numerical experiments" varying the "uncontrolled" parameters lead to the impression that the NQI best-fit parameters are virtually insensitive to variations of the empirical parameters within certain limits. The best-fit Euler angles listed in Table 3 are, therefore, quite reliable.

5. Discussion and Conclusions

Since it is generally accepted that the NQI-tensor of the remote imidazole nitrogen is strongly connected to the axis frame of the five-membered ring [11], the α and β Euler angles have an important structural implication. According to theoretical calculations and NQR experiments on imidazole compounds [20] the following assignment for the **Q**-axes is made: The z-axis is perpendicular to the imidazole plane, the x-axis is along the C-N-C bisector and the y-axis is perpendicular to these two. However, depending on the nature of the hydrogen bridge of the remote nitrogen, the axes of the **Q**-tensor corresponding with the largest principal values can be interchanged [21]. If we assume that the z-axis of the g-matrix is perpendicular to the plane of the directly coordinating nitrogens, we are able to determine the orientation of the imidazole plane in the metal complex, given a certain choice for the **Q**-axes. Also the choice for the $g_{\|}$ direction is not unambiguous, in particular for the Cu(II)-PMA complex: we can choose the $g_{\|}$ either along the axis connecting the copper ion to the axial nitrogen ligand or as the normal to the plane of the four coordinating equatorial nitrogens. The Euler angles α and β can now be related to the polar angles defining the orientation of the $g_{\|}$-vector in the quadrupole axes frame of the remote nitrogen atom in the imidazole ring. In Table 3 the best-fit angles α and β are compared with the corresponding values derived from the crystal structure [22]. Fig. 10 displays a schematic impression of the coordination structure of Cu(II)-PMA in which the Euler angle β is indicated. The angle β determined from the simulations correspond within the experimental error to the value derived from the crystal structure, for both Cu(II)-Pypep and Cu(II)-PMA. The values for α, however, shows a strong discrepancy. This discrepancy can be lifted to a great extent by interchanging the x- and y-axis of the **Q**-tensor in the imidazole ring, which will increase the value of a by 90°. Another possibility to explain this difference is to assume that the solution structure of both complexes deviates substantially from their crystal structure. Neither explanation is very satisfying for this discrepancy A single crystal study of both complexes in a diamagnetic host would seem the only way to resolve this problem.

In summary, we can conclude that the orientation of the imidazole ring in Cu(II)-BLM, Cu(II)-PMA and Cu(II)-Pypep seems to be very similar based on the Euler angles α and β (see Table 3). We have been able to obtain this structural information from a system with an axial g-matrix and a quadrupole tensor with a large asymmetry parameter thus making it impossible to resolve a

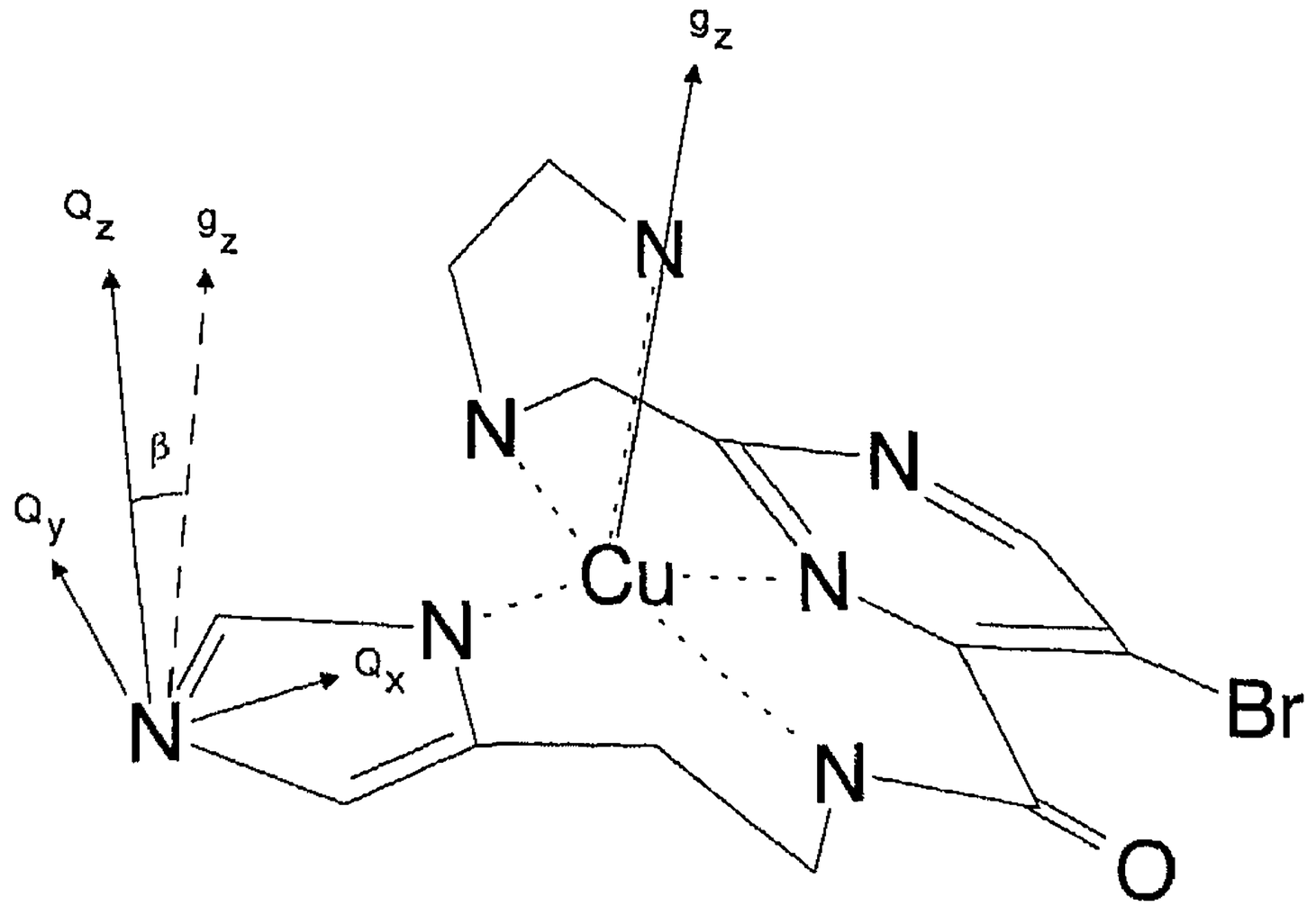

Fig. 10. A schematic drawing of the structure of Cu(II)-PMA. The *z*-axis of the *g*-matrix and the principal axis of the NQI tensor of the remote nitrogen of imidazole are indicated with arrows. The angle between the Q_z and the g_z axis is the Euler angle β.

complete tensor orientation. However with simulations and the use of model compounds we were able to obtain significant structural information about this disordered system.

The results of the model compounds are proof of the usefulness of the method of orientation selective ESEEM. Even with broad overlapping peaks the direct comparison of the measurement and simulation via the "inproduct method" makes it possible to fit these spectra.

Acknowledegements

The authors want to thank A. A. K. Klaassen and G. E. Janssen for their technical assistance and R. J. M. Klein-Gebbink of the Department of Organic Chemistry for his help in the synthesis of the PypepH ligand. This work was financed by the foundation for scientific research in the Netherlands (N.W.O.) and by a grant from the National Institute of Health (CA 53076).

References

[1] Stubbe J., Kozarich J.W.: Chem. Rev. **87**, 1107–1136 (1987)
[2] Umezawa H., Maeda K., Takeuchi T., Okami Y.: J. Antibiotic., Ser. A **19**, 200–209 (1966)
[3] Iitaka Y., Nakamura H., Nakatani T., Muraoka Y., Fuji A., Takita T., Umezawa H.: J. Antibiotics 31, 1070–1072 (1978)
[4] Akkerman M.A.J., Haasnoot C.A.G., Hilbers C.W.: Eur. J. Biochem. **173**, 221–225 (1988)
[5] Akkerman M.A.J., Haasnoot C.A.G., Hilbers C.W.: Magn. Reson. Chem. **26**, 793 (1988)
[6] Akkerman M.A.J., Neijman E.W., Wijmenga S.S., Hilbers C.W.: J. Am. Chem. Soc. **112**, 7462 (1990)

[7] Burger R.M., Adler A., Horwitz S.B., Peisach J.: Biochemistry **20**, 1701–1704 (1981)
[8] Brown S.J., Stephan D.W., Mascharak P.K.: J. Am. Chem. Soc. **110**, 1996–1997 (1988)
[9] Brown S.J., Tao X., Stephan D.W., Mascharak P.K.: Inorg. Chem. **25**, 3377–3384 (1986)
[10] Flanagan H.L., Gerfen G.J., Lai A., Singel D.J.: J. Chem. Phys. **88**, 2163–2168 (1988)
[11] Goldfarb D., Fauth J.-M., Farver O., Pecht I.: Appl. Magn. Reson. **3**, 333–351 (1992)
[12] Goldfarb D., Fauth J.-M., Tor Y., Shanzer A.: J. Am. Chem. Soc. **113**, 1941–1948 (1991)
[13] Shane J.J.: PhD Thesis. The Netherlands: University of Nijmegen 1993.
[14] Fauth J.-M., Schweiger A., Braunschweiler L., Ernst R.R.: J. Magn. Reson. **66**, 74–85 (1986)
[15] Flanagen H.L., Singel D.J.: J. Chem. Phys. **87**, 5606–5616 (1987)
[16] Reijerse E.J., Keijzers C.P.: J. Magn. Reson. **71**, 83 (1987)
[17] Mims W.: Phys. Rev. **5B**, 2409–2419 (1972)
[18] Mims W.: Phys. Rev. **6B**, 3543–3545 (1972)
[19] Keijzers C.P., Reijerse E.J., Stam P., Dumont M.F., Gribnau M.C.M.: J. Chem. Soc., Faraday Trans. **83**, 3493–3503 (1987)
[20] Palmer M.H., Scott F.E., Smith J.A.S.: Chem. Phys. **74**, 9–14 (1983)
[21] Colaneri M.J., Peisach J.: J. Am. Chem. Soc. **114**, 5335–5341 (1992)
[22] Brown S.J., Hudson S.E., Stephan D.W., Mascharak P.K.: Inorg. Chem. **28**, 468–477 (1989)

Author's address: Prof. Dr. Eduard J. Reijerse, Department of Molecular Spectroscopy, University of Nijmegen, Toernooiveld 1, 6525 ED Nijmegen, The Netherlands